NATIONAL AERONAUTICS AND SPACE ADMINISTRATION

Technical Report No. 32-665

Ranger Photometric Calibration

G. M. Smith
D. E. Willingham

JET PROPULSION LABORATORY
CALIFORNIA INSTITUTE OF TECHNOLOGY
PASADENA, CALIFORNIA
August 15, 1965

NATIONAL AERONAUTICS AND SPACE ADMINISTRATION

Technical Report No. 32-665

Ranger Photometric Calibration

G. M. Smith
D. E. Willingham

R. L. Heacock, *Manager*
Lunar and Planetary Instruments Section

JET PROPULSION LABORATORY
CALIFORNIA INSTITUTE OF TECHNOLOGY
PASADENA, CALIFORNIA

August 15, 1965

Prepared Under Contract No. NAS 7-100
National Aeronautics & Space Administration

CONTENTS

TABLES

FIGURES

ABSTRACT

34216

An equation is derived which relates collimator luminance values as read with a Pritchard photometer to actual lunar scene luminance values, such that identical *Ranger* camera response occurs. The solution of this equation requires detailed knowledge of emission spectra of the Moon, the collimator, and a calibration standard and the spectral response characteristics of the "standard eye," the photometer, and each specific vidicon camera. Calculations are made for six typical *Ranger* cameras, and variations in the results from camera to camera are noted.

Author

I. INTRODUCTION

Photometric calibration of a space photographic system is an important requirement for missions such as *Ranger* and *Mariner* if the full potential of the photographic data is to be realized. Calibration is required for both absolute and relative luminance measurements which yield topographic information when used in conjunction with the known photometric characteristics of the scene. The determination of correct shutter exposure times and camera dynamic range also require accurate photometric calibration.

In principle, the simplest method of calibration is to use a source of illumination which has the correct spectral characteristics to illuminate the camera and then to determine system output as a function of the source intensity. In practice, however, it is difficult to obtain a source with sufficient intensity that has the proper spectral characteristics. Because of this difficulty, a method has been developed which allows the use of a source that does not simulate the spectral distribution of the scene exactly. This method includes the calculation of a correction factor which accounts for the difference between the actual scene and the calibration source.

Photovisual units are used in the development of the correction factor, since the measured lunar data are in photovisual units. The method, however, is not limited to those units.

The calculation of the correction factor requires the following measured characteristics:

1. Spectral response of the camera
2. Spectral response of the photometer used for the luminance measurements
3. Spectral emission of the calibration sources
4. Spectral emission of the scene to be photographed
5. Spectral emission of a 100-ft-L reference source.

Two types of sources are used in the *Ranger* calibration. One is a collimator focused at infinity, which gives an image in the camera focal plane. The other is a diffuse source, which is placed close to the camera lens and does not give a real image. The illumination at the image plane is slightly nonuniform with the diffuse source; however, measurements have been made to account for nonuniformity.

II. DERIVATION

Suppose a camera viewing a lunar scene gives an output E in millivolts. Now, suppose that a calibration source is adjusted so that the camera again has E mv output when viewing the source. If the scene luminance is known in foot-lamberts (photovisual units) and if the collimator luminance is then measured with a photometer, which has a different spectral response from the cameras, a difference in the two luminance values will exist. This difference is caused by the differences in the spectral emission of the calibration source and the Moon. Thus, for identical camera system output, the calibration source must be set to an indicated luminance which is different from the true luminance of the lunar scene. This indicated luminance, as measured by the photometer, is expressed as

$$B_c = \int_0^\infty A P_r(\lambda)\, k_2 C_r(\lambda)\, d\lambda \tag{1}$$

where B_c is the measured collimator luminance (in ft-L), $P_r(\lambda)$ is the photometer relative spectral response, $C_r(\lambda)$ is the relative calibration source spectral emission, and A and k_2 are the photometer and calibration-source scale factors which are to be determined.

The photometer scale factor A is obtained by use of a primary 100-ft-L reference source for the photometer in the following manner. When viewing the reference source, the photometer scale factor (gain) is adjusted so that the output meter reads 100 ft-L. Therefore,

$$\int_0^\infty A P_r(\lambda)\, k_1 R_r(\lambda)\, d\lambda = 100\,\text{ft-L} \tag{2}$$

where $R_r(\lambda)$ is the relative spectral emission of the reference source and k_1 the amplitude.

To determine k_1, it is necessary to make use of the definition of the photovisual units. The luminous portion of the radiated energy is defined as that portion within the standard eye response $I_r(\lambda)$. This standard eye response has been adopted as the ICI photopic luminosity function. For the reference source, one has

$$\int_0^\infty I_r(\lambda)\, k_1 R_r(\lambda)\, d\lambda = 100\,\text{ft-L} \tag{3}$$

where $I_r(\lambda)$ and $R_r(\lambda)$ are, of course, known. Therefore, from Eqs. (2) and (3), we have

$$A = \frac{\int_0^\infty I_r(\lambda)\, R_r(\lambda)\, d\lambda}{\int_0^\infty P_r(\lambda)\, R_r(\lambda)\, d\lambda} \tag{4}$$

It now remains to determine k_2 in Eq. (1). The key relationship required is that the vidicon output must be the same for both the calibration source and the lunar emission; i.e.,

$$\int_0^\infty V_r(\lambda)\, k_2 C_r(\lambda)\, d\lambda = \int_0^\infty V_r(\lambda)\, k_3 M_r(\lambda)\, d\lambda \tag{5}$$

where $V_r(\lambda)$ is the relative vidicon spectral response, $M_r(\lambda)$ is the relative lunar emission spectrum, and k_3 is the lunar emission scale factor. The scale factor k_3 may be obtained by noting that the lunar scene luminance B_M is

$$B_M = \int_0^\infty I_r(\lambda)\, k_3 M_r(\lambda)\, d\lambda$$

Solving for k_3 and substituting into Eq. (5), we have

$$k_2 = \frac{B_M \int_0^\infty V_r(\lambda)\, M_r(\lambda)\, d\lambda}{\int_0^\infty V_r(\lambda)\, C_r(\lambda)\, d\lambda \int_0^\infty I_r(\lambda)\, M_r(\lambda)\, d\lambda} \tag{6}$$

Substituting Eqs. (4) and (6) into (1) gives the desired result:

$$\frac{B_c}{B_M} = \frac{\int_0^\infty I_r(\lambda) R_r(\lambda) d\lambda \int_0^\infty V_r(\lambda) M_r(\lambda) d\lambda \int_0^\infty P_r(\lambda) C_r(\lambda) d\lambda}{\int_0^\infty P_r(\lambda) R_r(\lambda) d\lambda \int_0^\infty V_r(\lambda) C_r(\lambda) d\lambda \int_0^\infty I_r(\lambda) M_r(\lambda) d\lambda} \tag{7}$$

Hereafter, the right side of Eq. (7) will be denoted as the collimator correction factor.

III. DATA COLLECTION

For the evaluation of Eq. (7), the spectral emission or response of the reference source, Moon, calibration source, photometer, standard eye, and vidicon are required.

The most difficult of the above to measure are the vidicon and photometer responses, since these involve electronic systems as well as photosensitive surfaces as primary sensors. Further, the vidicon response is nonlinear (i.e., slope of output voltage vs. luminance is not constant) and thus requires care in measurement. A description of the measurement technique follows.

The vidicon voltage output in the linear region can be described by

$$E = k_G \left[\int_0^\infty V(\lambda)\, B(\lambda)\, d\lambda \right]^\gamma$$

where k_G is the proportionality or gain constant, $V(\lambda)$ is the vidicon spectral response function, $B(\lambda)$ is the source distribution function, and γ is a vidicon constant independent of wavelength. When using a monochromatic source,

$$\int_0^\infty V(\lambda)\, B(\lambda)\, d\lambda \simeq V(\lambda_i)\, B(\lambda_i)\, \Delta\lambda$$

where $B(\lambda_i)$ is the average source magnitude over the wavelength interval $\Delta\lambda$, centered at wavelength λ_i.

The wavelength at which the camera is most sensitive is first determined, and a voltage in the linear region is chosen such that

$$E_o = k_G [V(\lambda_o)\, B(\lambda_o)\, \Delta\lambda]^\gamma \tag{8}$$

If a new source wavelength is selected and the source intensity varied to give constant vidicon voltage output, then

$$E_o = k_G [V(\lambda_o)\, B(\lambda_o)\, \Delta\lambda]^\gamma = k_G [V(\lambda_i)\, B(\lambda_i)\, \Delta\lambda]^\gamma$$

or

$$\frac{V(\lambda_i)}{V(\lambda_o)} = \frac{B(\lambda_o)}{B(\lambda_i)} \tag{9}$$

The quantity $B(\lambda_i)\, \Delta\lambda$ is easily measured with a photomultiplier tube and meter. Using the previous terminology, then,

$$\frac{V(\lambda_i)}{V(\lambda_o)} = V_r(\lambda_i) \tag{10}$$

where $V_r(\lambda_i)$ are discrete points of the vidicon relative response $V_r(\lambda)$.

Experimental measurements were made by RCA on several of the *Ranger* cameras, two of which were flown on *Ranger VII*. The experimental setup is shown in Fig. 1, the data are presented in Table 1, and fitted curves are shown in Figs. 2–7.

Table 1. Vidicon fitted curves

λ	P_1 Serial No. 031/028	P_2 Serial No. 022/022	P_3 Serial No. 021/039	P_4 Serial No. 016/016	F_A Serial No. 026/026	F_B Serial No. 017/017
350	0	0	0	—	0	0
360	0	0	0	0.055	0	0.010
370	0	0.023	0.005	0.061	0.010	0.022
380	0.058	0.057	0.018	0.069	0.045	0.040
390	0.135	0.094	0.032	0.081	0.087	0.062
400	0.188	0.135	0.050	0.097	0.133	0.086
410	0.254	0.178	0.071	0.120	0.190	0.115
420	0.318	0.227	0.103	0.150	0.249	0.150
430	0.382	0.280	0.137	0.187	0.314	0.190
440	0.448	0.340	0.180	0.225	0.387	0.235
450	0.507	0.405	0.229	0.270	0.460	0.286
460	0.568	0.472	0.289	0.322	0.538	0.344
470	0.630	0.542	0.358	0.379	0.612	0.410
480	0.694	0.613	0.440	0.439	0.682	0.480
490	0.751	0.682	0.520	0.507	0.754	0.551
500	0.805	0.753	0.620	0.580	0.820	0.622
510	0.850	0.821	0.710	0.656	0.880	0.692
520	0.894	0.880	0.786	0.737	0.935	0.759
530	0.929	0.929	0.856	0.824	0.980	0.827
540	0.960	0.970	0.918	0.898	1.000	0.885
550	0.985	1.000	0.968	0.944	0.965	0.944
560	1.000	0.997	1.000	0.972	0.902	0.992
570	0.964	0.983	1.000	0.987	0.828	1.000
580	0.917	0.960	0.960	0.992	0.756	0.969
590	0.862	0.932	0.900	0.987	0.683	0.909
600	0.805	0.899	0.842	0.970	0.610	0.818
610	0.743	0.855	0.778	0.936	0.538	0.705
620	0.676	0.805	0.710	0.887	0.463	0.600
630	0.611	0.742	0.640	0.829	0.400	0.517
640	0.540	0.665	0.573	0.765	0.328	0.441
650	0.470	0.585	0.502	0.688	0.260	0.377
660	0.403	0.510	0.440	0.605	0.205	0.323
670	0.342	0.423	0.370	0.511	0.160	0.275
680	0.286	0.340	0.308	0.430	0.125	0.232
690	0.235	0.255	0.250	0.358	0.096	0.191
700	0.190	0.182	0.200	0.298	0.073	0.157
710	0.152	0.129	0.158	0.245	0.052	0.124
720	0.128	0.089	0.124	0.198	0.037	0.099
730	0.090	0.062	0.098	0.159	0.029	0.075
740	0.068	0.048	0.075	0.125	0.022	0.057
750	0.052	0.040	0.061	0.097	0.017	0.042
760	0.038	0.035	0.047	0.072	0.011	0.035
770	0.029	0.031	0.035	0.053	0.007	0.028
780	0.022	0.027	0.026	0.037	0.003	0.021
790	0.017	0.026	0.018	0.026	0	0.016
800	0.011	0.024	0.008	0.019	0	0.010

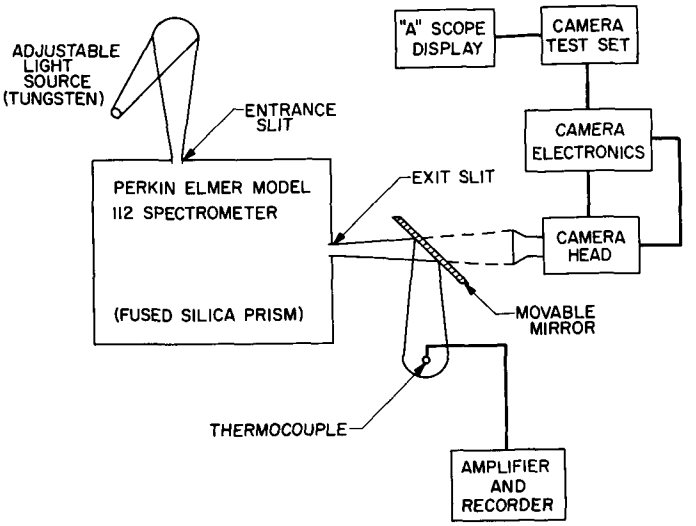

Fig. 1. RCA experimental setup vidicon spectral response

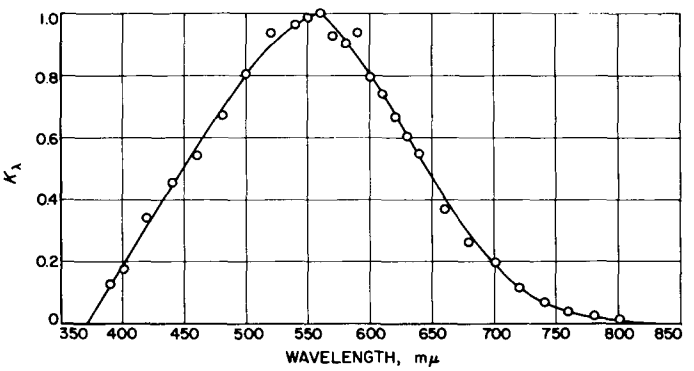

Fig. 2. P_1-camera vidicon plus lens (Serial No. 031/028)

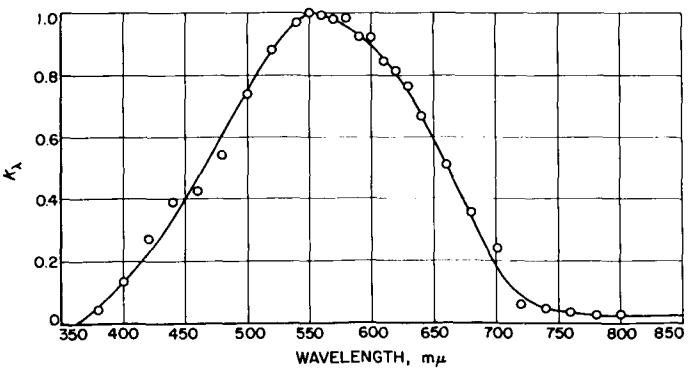

Fig. 3. P_2-camera vidicon plus lens (Serial No. 022/022)

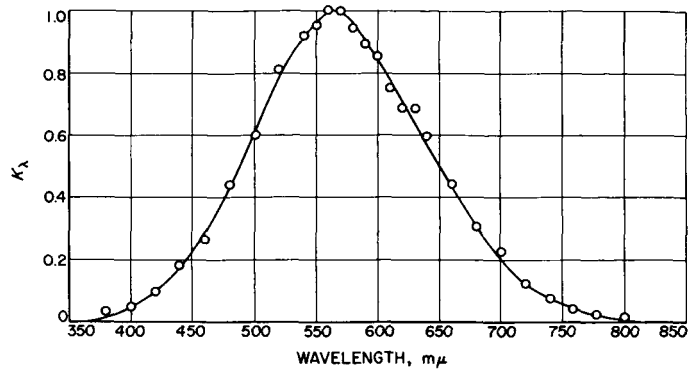

Fig. 4. P_3-camera vidicon plus lens (Serial No. 021/039)

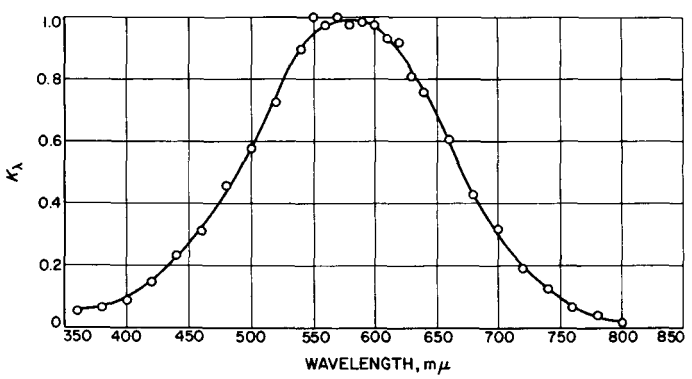

Fig. 5. P_4-camera vidicon plus lens (Serial No. 016/016)

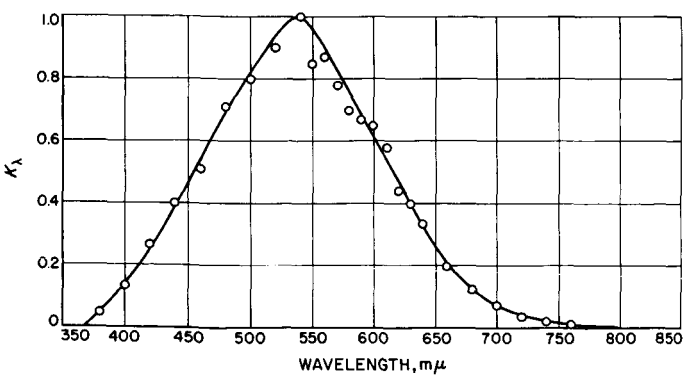

Fig. 6. F_A-camera vidicon plus lens (Serial No. 026/026)

Since the photometer is a linear device ($\gamma = 1.0$), a constant input energy at various wavelengths may be used to stimulate the photometer and the resultant voltage recorded. The experimental setup used in this case is shown in Fig. 8. The photometer was a Pritchard photometer, and its response was obtained at two gain settings, resulting in the two slightly different curves (Fig. 9). The curve denoted as P_{r1} was used for calculation purposes.

Fig. 7. F_B-camera vidicon plus lens (Serial No. 017/017)

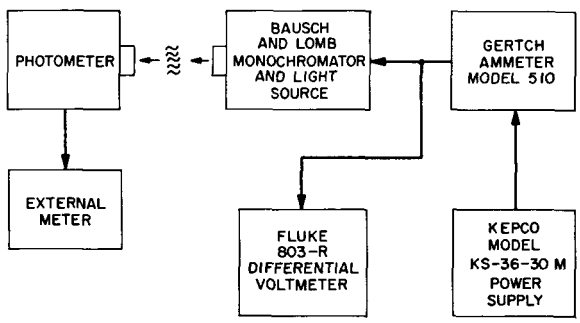

Fig. 8. Experimental setup photometer measurements

As mentioned in Section I, two types of calibration sources are used—collimators and an extended field source. Various luminance values were obtained during calibration by inserting neutral density filters in front of the collimators. Curves A through H of Fig. 10 show the spectral emission data for the two collimators and combinations of neutral density filters used in the *Ranger* calibrations. Curves E and H represent the collimator extremes and will be denoted as $C_{CE}(\lambda)$ and $C_{CH}(\lambda)$ in the calculations. The extended-field-source emission spectrum is shown in Fig. 11 and will be denoted as $C_F(\lambda)$. (Note that the "relative" subscript r has been dropped.)

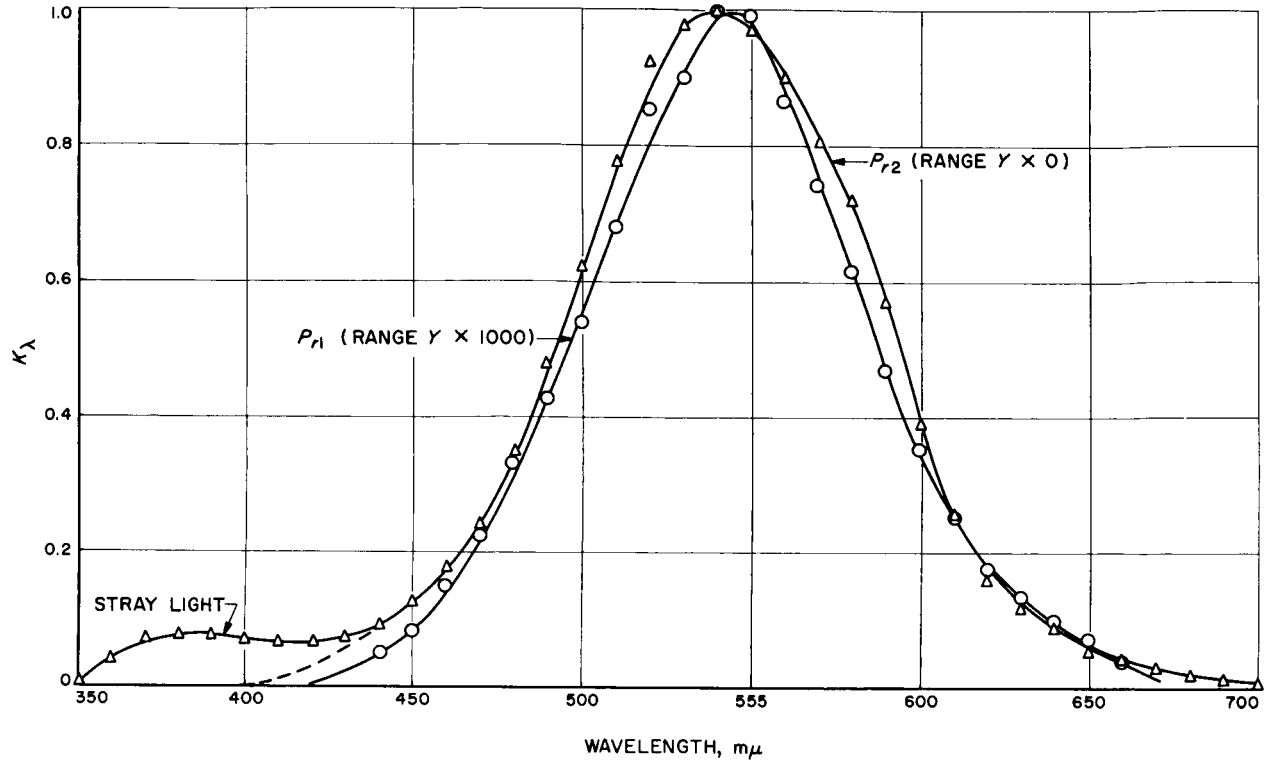

Fig. 9. Spectral sensitivity characteristics; Pritchard photometer (Serial No. 124)

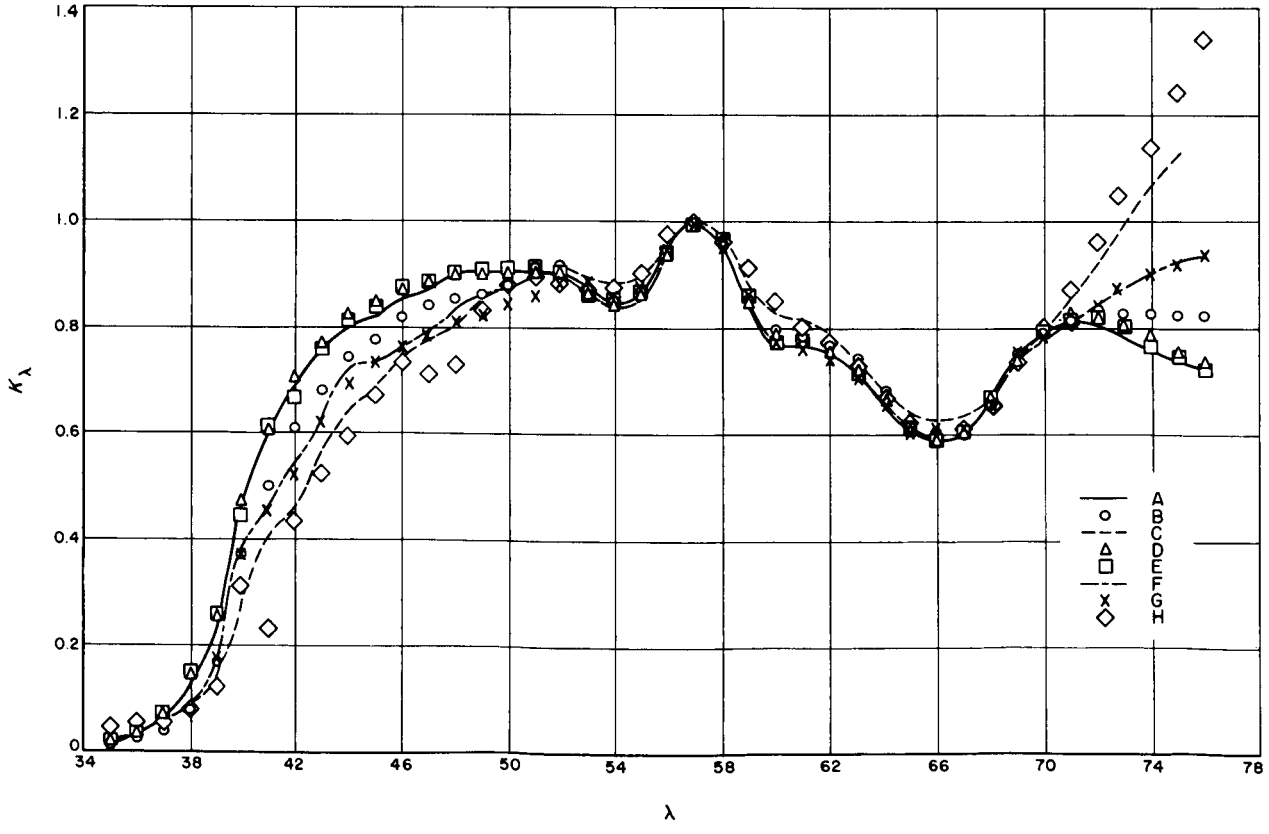

Fig. 10. Collimator spectral emission data

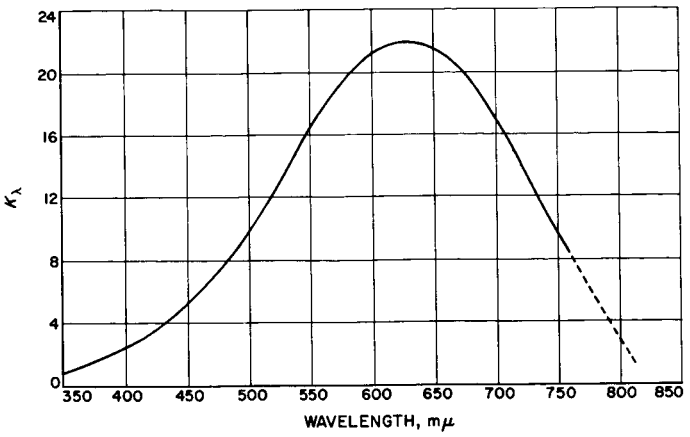

Fig. 11. Relative spectral emission, extended field source

The photopic luminosity curve and primary reference source (2854°K black body) are tabulated functions and are easily obtainable.

The lunar emission spectrum can be obtained by point-by-point multiplication of the Johnson solar curve $S_r(\lambda)$ and the lunar reflectance curve $A(\lambda)$ (Fig. 12).* In general, the Moon exhibits very little color variation, so that the resultant emission spectrum can be applied to nearly every area of the lunar surface.

The data for each of the spectra, except for the vidicon data, are listed in Table 2.

*Data for the latter curve were obtained from Ewen A. Whitaker of the Lunar and Planetary Laboratory, University of Arizona.

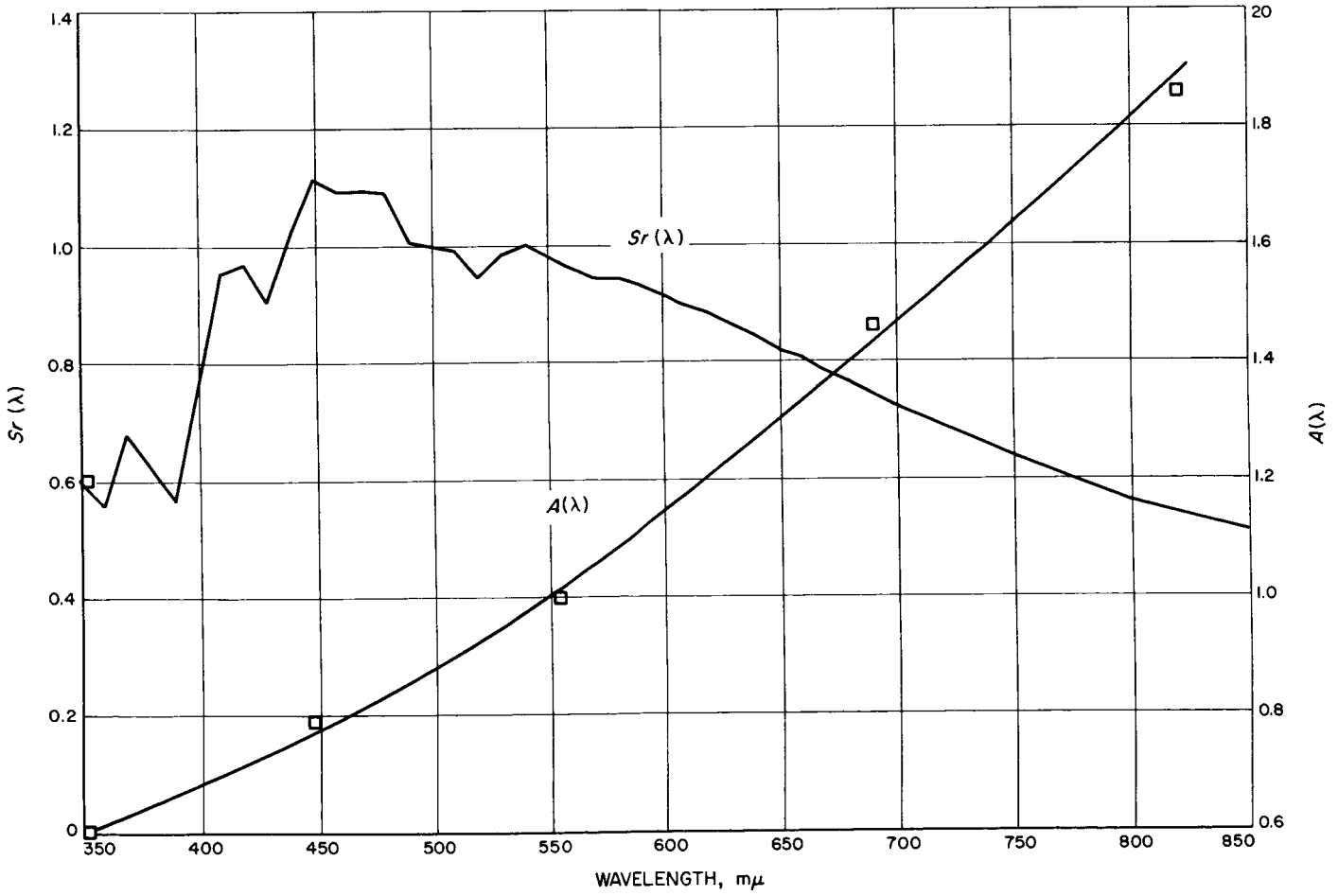

Fig. 12. Johnson solar curve and lunar reflectance

Table 2. Response and emission data

λ	R_r	I_r	P_{r1}	P_{r2}	A	S_r	M_r	C_{CE}	C_{CH}
350					0.600			0.0252	0.0474
360					0.613			0.0401	0.0547
370					0.628	0.675	0.4239	0.0755	0.0591
380		0.0000			0.644	0.620	0.3993	0.1524	0.0818
390	0.12086	0.0001			0.660	0.568	0.3749	0.2624	0.1255
400	0.14709	0.0004		0.000	0.678	0.777	0.5268	0.4482	0.1960
410	0.17676	0.0012		0.018	0.696	0.949	0.6605	0.6189	0.2920
420	0.20996	0.0040	0.000	0.038	0.715	0.970	0.6936	0.6694	0.410
430	0.24672	0.0116	0.019	0.060	0.734	0.900	0.6606	0.7563	0.5210
440	0.28704	0.0230	0.050	0.090	0.753	1.030	0.7756	0.8126	0.5980
450	0.33087	0.0380	0.085	0.129	0.775	1.110	0.8602	0.8347	0.6729
460	0.37813	0.0600	0.150	0.178	0.795	1.090	0.8666	0.8815	0.7356
470	0.42870	0.0910	0.211	0.248	0.816	1.092	0.8911	0.8861	0.7165
480	0.48244	0.1390	0.309	0.340	0.837	1.090	0.9123	0.9032	0.7329
490	0.53914	0.2080	0.428	0.476	0.859	1.010	0.8676	0.9111	0.8392
500	0.59862	0.3230	0.562	0.617	0.880	1.000	0.8800	0.9136	0.8831
510	0.66064	0.5030	0.685	0.768	0.901	0.990	0.8920	0.9149	0.8973
520	0.72497	0.7100	0.812	0.840	0.926	0.944	0.8741	0.9057	0.8839
530	0.79133	0.8620	0.918	0.981	0.950	0.985	0.9358	0.8714	0.8753
540	0.85947	0.9540	0.991	1.000	0.977	1.000	0.9770	0.8531	0.8776
550	0.92912	0.9950	0.972	0.969	1.002	0.987	0.9890	0.8735	0.9074
560	1.0000	0.9950	0.880	0.900	1.030	0.960	0.9888	0.9374	0.9780
570	1.0718	0.9520	0.748	0.810	1.059	0.945	1.0008	1.0000	1.0000
580	1.1444	0.8700	0.602	0.700	1.087	0.946	1.0283	0.9724	0.9702
590	1.2173	0.7570	0.458	0.510	1.115	0.930	1.0370	0.8648	0.9145
600	1.2904	0.6310	0.340	0.390	1.144	0.917	1.0490	0.7746	0.8510
610	1.3634	0.5030	0.253	0.245	1.173	0.895	1.0498	0.7738	0.8070
620	1.4362	0.3810	0.178	0.170	1.203	0.880	1.0586	0.7563	0.7785
630	1.5083	0.2650	0.127	0.118	1.234	0.860	1.0612	0.7225	0.7340
640	1.5798	0.1750	0.089	0.083	1.266	0.840	1.0634	0.6686	0.6773
650	1.6502	0.1070	0.051	0.058	1.298	0.817	1.0605	0.6173	0.6278
660	1.7196	0.0610	0.038	0.040	1.330	0.806	1.0720	0.5985	0.6036
670	1.7876	0.0320	0.016	0.026	1.361	0.781	1.0629	0.6123	0.6096
680	1.8542	0.0170	0.002	0.017	1.395	0.765	1.0672	0.6728	0.6572
690	1.9193	0.0082	0.000	0.010	1.429	0.743	1.0617	0.7492	0.7369
700	1.9826	0.0041		0.009	1.462	0.720	1.0526	0.7984	0.8023
710	2.0440	0.0021			1.496	0.707	1.0577	0.8168	0.8700
720	2.1036	0.0010			1.531	0.690	1.0564	0.8143	0.9390
730	2.1611	0.0005			1.564	0.672	1.0510	0.8013	1.0030
740	2.2166	0.0003			1.600	0.655	1.0480	0.7692	1.0680
750	2.2699	0.0001			1.635	0.639	1.0448	0.7442	1.1250
760	2.3211	0.0001			1.670	0.624	1.0421	0.7250	1.1870
770	2.3700	0.0000			1.706	0.608	1.0372	0.7180	1.2430
780					1.742	0.591	1.0295	0.7110	1.2980
790					1.778	0.578	1.0277	0.7090	1.3500
800					1.812	0.560	1.0147	0.7080	1.4000

IV. RESULTS AND CONCLUSIONS

Values for each of the integrals making up the overall correction-factor calculations are given in Table 3. As three calibration source curves have been noted, calculations for each vidicon camera will result in three correction factors. These factors are listed below for each camera.

Camera	Serial No.	Correction Factors $C_{CE}(\lambda)$	$C_{CH}(\lambda)$	$C_F(\lambda)$
P_1	031/028	1.178	1.209	1.133
P_2	022/022	1.200	1.217	1.088
P_3	021/039	1.208	1.202	1.053
P_4	016/016	1.238	1.229	1.048
F_A	026/026	1.139	1.180	1.169
F_B	017/017	1.185	1.213	1.080

The collimator source $C_{CE}(\lambda)$ applies for those cases in which few neutral density filter layers are inserted in the collimator field; i.e., for high light levels. The collimator source $C_{CH}(\lambda)$ is applicable for the lower light levels. However, within the photometric accuracy of the overall system, one can use an average correction factor of 1.20 for the collimators in nearly every case. The correction factors for $C_F(\lambda)$ apply for those instances in which the extended field source is used as a stimulus.

Cameras P_1 and P_3 were flown on *Ranger VII*, and the above calculations were used in deriving light transfer functions for use in absolute photometry studies and impact point selection.

Table 3. Values of integrals*

$\int_0^\infty V_{r_{P_1}}(\lambda)\, M_r(\lambda)\, d\lambda$	19.0117	$\int_0^\infty V_{r_{P_1}}(\lambda)\, C_{CH}(\lambda)\, d\lambda$	16.0200
$\int_0^\infty V_{r_{P_2}}(\lambda)\, M_r(\lambda)\, d\lambda$	19.3119	$\int_0^\infty V_{r_{P_2}}(\lambda)\, C_{CH}(\lambda)\, d\lambda$	16.1638
$\int_0^\infty V_{r_{P_3}}(\lambda)\, M_r(\lambda)\, d\lambda$	17.0705	$\int_0^\infty V_{r_{P_3}}(\lambda)\, C_{CH}(\lambda)\, d\lambda$	14.4624
$\int_0^\infty V_{r_{P_4}}(\lambda)\, M_r(\lambda)\, d\lambda$	19.4081	$\int_0^\infty V_{r_{P_4}}(\lambda)\, C_{CH}(\lambda)\, d\lambda$	16.0809
$\int_0^\infty V_{r_{F_A}}(\lambda)\, M_r(\lambda)\, d\lambda$	15.6262	$\int_0^\infty V_{r_{F_A}}(\lambda)\, C_{CH}(\lambda)\, d\lambda$	13.4880
$\int_0^\infty V_{r_{F_B}}(\lambda)\, M_r(\lambda)\, d\lambda$	16.1648	$\int_0^\infty V_{r_{F_B}}(\lambda)\, C_{CH}(\lambda)\, d\lambda$	13.5678
$\int_0^\infty V_{r_{P_1}}(\lambda)\, C_{CE}(\lambda)\, d\lambda$	16.5434	$\int_0^\infty V_{r_{P_1}}(\lambda)\, C_F(\lambda)\, d\lambda$	288.274
$\int_0^\infty V_{r_{P_2}}(\lambda)\, C_{CE}(\lambda)\, d\lambda$	16.4984	$\int_0^\infty V_{r_{P_2}}(\lambda)\, C_F(\lambda)\, d\lambda$	304.801
$\int_0^\infty V_{r_{P_3}}(\lambda)\, C_{CE}(\lambda)\, d\lambda$	14.4811	$\int_0^\infty V_{r_{P_3}}(\lambda)\, C_F(\lambda)\, d\lambda$	278.359
$\int_0^\infty V_{r_{P_4}}(\lambda)\, C_{CE}(\lambda)\, d\lambda$	16.0720	$\int_0^\infty V_{r_{P_4}}(\lambda)\, C_F(\lambda)\, d\lambda$	318.217
$\int_0^\infty V_{r_{F_A}}(\lambda)\, C_{CE}(\lambda)\, d\lambda$	14.0632	$\int_0^\infty V_{r_{F_A}}(\lambda)\, C_F(\lambda)\, d\lambda$	229.700
$\int_0^\infty V_{r_{F_B}}(\lambda)\, C_{CE}(\lambda)\, d\lambda$	13.9893	$\int_0^\infty V_{r_{F_B}}(\lambda)\, C_F(\lambda)\, d\lambda$	257.053
$\int_0^\infty I_r(\lambda)\, R_r(\lambda)\, d\lambda$	10.7895	$\int_0^\infty I_r(\lambda)\, M_r(\lambda)\, d\lambda$	10.5080
$\int_0^\infty P_{r_1}(\lambda)\, C_{CE}(\lambda)\, d\lambda$	8.8488	$\int_0^\infty P_{r_1}(\lambda)\, C_F(\lambda)\, d\lambda$	148.267
$\int_0^\infty P_{r_1}(\lambda)\, C_{CH}(\lambda)\, d\lambda$	8.7912	$\int_0^\infty P_{r_1}(\lambda)\, R_r(\lambda)\, d\lambda$	8.8635

*Values obtained by numerical integration.